

## Electrical, structural, and superconducting properties of hydrogenated Nb-Ta superlattices

Ctirad Uher and Joshua L. Cohn

*Physics Department, University of Michigan, Ann Arbor, Michigan 48109-1120*

Paul F. Miceli and Hartmut Zabel

*Department of Physics and Materials Research Laboratory, University of Illinois at Urbana, Urbana, Illinois 61801*

(Received 5 March 1987)

The electrical resistivity and superconducting transition temperatures are studied as a function of hydrogen content on two series of Nb-Ta superlattices grown by molecular-beam epitaxy with modulation wavelengths of 20 and 85 Å. Hydrogen enhances the resistivity of the structures which, in extreme cases, leads to a logarithmic temperature dependence at very low temperatures. All structures undergo a transition to a superconducting state, but with increasing hydrogen content the transition temperatures are continuously depressed. This behavior differs from that of bulk hydrogenated Nb and Ta systems and is believed to have its origin in the epitaxial constraints imposed by the substrate on these single-crystalline superlattices.

Recent advances in ultrahigh-vacuum (UHV) deposition techniques such as molecular-beam epitaxy have opened new avenues for the study of hydrogenation in thin films and artificial metallic superlattices. The presence of a host-metal compositional modulation can be expected to have a profound effect on the physical and thermodynamic properties of the interstitial hydrogen lattice gas. The first investigation of such a system has been undertaken recently by Miceli, Zabel, and Cunningham,<sup>1</sup> who observed a hydrogen-induced strain modulation in single-crystalline Nb-Ta superlattices. In addition to the Curie-Weiss behavior for a hydrogen-concentration modulation they also noted a far greater solubility of hydrogen in the Nb-Ta superlattice from what would be expected for bulk Nb or Ta.

In this work we have investigated the effect of hydrogen loading on the carrier transport and superconductivity in Nb-Ta superlattices. Measurements were made on two series of Nb-Ta superlattices of modulation wavelength 20 and 85 Å grown by molecular-beam epitaxy on (11 $\bar{2}$ 0) sapphire substrates with [110] film orientation. The tantalum fraction in these two series is 0.6 and 0.17, respectively, and is chosen so that the Ta spacer is roughly the same in both sets of samples ( $d_{\text{Ta}}=12$  and 14 Å, respectively). Hydrogen loading was performed<sup>1</sup> *in situ* in a high-vacuum x-ray furnace where the lattice expansion due to the dissolved hydrogen could be monitored. Since we cannot directly measure the hydrogen concentration, the lattice expansion determined from x-ray diffraction can be converted to a hydrogen concentration. As we shall discuss, it is found that this lattice expansion occurs only in the direction normal to the plane of the film, a consequence of the epitaxial constraints imposed by the substrate. In an unconstrained bulk metal, the relationship between volume expansion and hydrogen concentration is given by<sup>2</sup>

$$\Delta V/V = 3\Delta a/a = c_H(\Delta v/\Omega), \quad (1)$$

where  $a$  is the lattice parameter,  $c_H$  is the hydrogen concentration (H-atom-to-metal-atom ratio),  $\Delta v$  is the

volume change per hydrogen atom, and  $\Omega$  is the volume of a host-metal atom. For the present one-dimensional expansion, we estimate  $c_H$  from Eq. (1) with  $\Delta V/V = \Delta a/a$  and  $\Delta v/\Omega = 0.165$ , the average value for the bulk metal-hydrogen systems.<sup>2</sup> Some relevant parameters of the samples studied are presented in Table I.

Experimental data on the electrical resistivity measured parallel to the deposited layers are shown in Figs. 1(a) and 1(b). For all of our samples current densities were 5–10 A/cm<sup>2</sup>. We first describe the behavior of the two hydrogen-free Nb-Ta superlattices,  $\Lambda = 20$  Å and  $\Lambda = 85$  Å, the room-temperature resistivities of which are 23.8 and 18.9  $\mu\Omega$  cm, respectively. These values are to be compared with the bulk resistivities<sup>3</sup> of Nb and Ta of 14.5 and 13.1  $\mu\Omega$  cm. The resistivities have a metallic character throughout the temperature range above the superconducting transitions. The residual resistivity ratios (RRR's), defined as  $\rho_{300\text{K}}/\rho_{10\text{K}}$ , are 4.6 and 12.3 for the two hydrogen-free superlattices. Taking the mean free path<sup>4</sup> (MFP) of bulk Nb and Ta at 300 K as 26 Å, the data imply low-temperature MFP's of 75 and 240 Å, respectively. These values are about a factor of 3 to 4 times larger than the modulation wavelength and reflect a relatively high quality of interfaces in these superlattices.

Superconducting transition temperatures of the two hydrogen-free Nb-Ta superlattices are 8.08 K ( $\Lambda = 85$  Å)

TABLE I. Some relevant parameters of the Nb-Ta superlattices.

$\Lambda$ (Å)	$\Delta V/V$	$\rho(295\text{ K})$ ( $\mu\Omega$ cm)	RRR	MFP (above $T_c$ ) (Å)	$T_c$ (K)
20	0	23.8	4.60	75	7.67
	0.05	93.6	1.33	5	3.19
	0.08	122	1.23	4	0.52
85	0	18.9	12.3	240	8.08
	0.013	44.1	1.97	16	5.76
	0.06	92.9	1.40	5	3.09

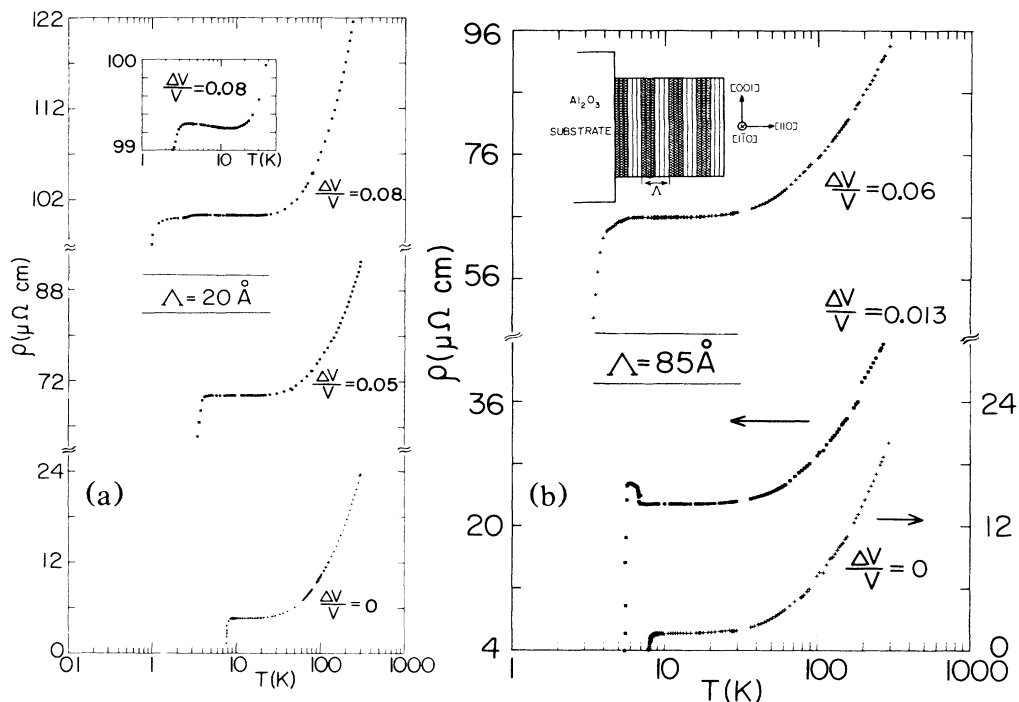


FIG. 1. (a) Temperature dependence of resistivity of pure and hydrogenated Nb-Ta superlattices with the modulation wavelength of 20 Å. Hydrogen content expressed as a volume change  $\Delta V/V$ . The inset shows a regime of a negative temperature coefficient of resistivity observed on the most heavily loaded sample at low temperatures. (b) Temperature-dependent resistivity of pure and hydrogenated Nb-Ta superlattices with the modulation wavelength of 85 Å. Crystallographic orientation of the structure is shown in the inset.

and 7.67 K ( $\Lambda=20$  Å). The structures are clearly proximity-coupled systems, the reduction of  $T_c$  from the bulk Nb value of 9.3 K being due to the lower  $T_c$  (4.4 K) of the Ta spacer. A small reduction in  $T_c$  on the 20-Å-modulation-wavelength sample in comparison to the 85-Å structure is, no doubt, associated with extremely thin Nb layers,<sup>5,6</sup> representing nominally no more than four monolayers. Furthermore, one must allow for some degree of interdiffusion between Nb and Ta layers. This would be particularly relevant to our very-small-modulation-wavelength structure of 20 Å, since the typical extent of interdiffusion in Nb-Ta superlattices is estimated<sup>7</sup> as 4.5 Å. The width of the superconducting transitions, defined here as a temperature difference corresponding to 10% and 90% resistance values, is 0.03 K for the 85-Å structure and a much larger 0.061 K for the 20-Å structure. This, again, is in accord with a generally accepted view that disorder leads to broadening of superconducting transitions.

We now address the effect of hydrogenation of these structures. X-ray diffraction experiments on Nb-Ta superlattices and Nb thin films with interstitially dissolved hydrogen reveal a one-dimensional lattice expansion normal to the film—a result which is in contrast to bulk metal-hydrogen systems where the lattice expansion has cubic symmetry in the single-phase region of the phase diagram. We observe this behavior, in general, for the samples used in these transport studies as well as for other Nb-Ta superlattices and Nb films<sup>8</sup> having total film thick-

ness ranging from 2000 to 5500 Å. Figure 2 shows x-ray diffraction peaks both parallel and perpendicular to the film normal for the 85-Å superlattice containing hydrogen ( $\Delta V/V=0.013$ ). It can be seen that the in-plane peaks display the pristine-lattice parameter for the hydrogen-free metal (Nb and Ta have the same pristine-lattice parameter). Evidently, the substrate constrains the lattice from expanding in the plane of the film. The one-dimensional expansion is found to occur up to a maximum value of  $(\Delta d/d)_{\max} \sim 0.016 (\pm 0.003)$ . Above this value, a precipitation of several metal-hydrogen phases takes place, as evidenced by the appearance of multiple Bragg peaks along each of the three orthogonal reciprocal-lattice directions [see inset in Fig. 1(b)]. Evaluating the total volume expansion from these, we find that each precipitate exhibits essentially the same  $\Delta V/V$ . The magnitude of the volume expansion is much smaller than would be expected from bulk metal-hydride phases, therefore the observed precipitates differ only by their structural relations to the substrate but not by their hydrogen concentration. This behavior is evidently the result of the interaction between the film and the substrate.

Hydrogen loading also has a dramatic effect on both the electrical resistivity and the superconducting transition temperature. This is clearly evident from a strongly enhanced resistivity and depressed superconducting transition temperature as shown in Figs. 1(a) and 1(b). We estimate that the electrical resistivity at ambient temperature rises by about 0.75  $\mu\Omega$  cm per at. % H interstitial im-

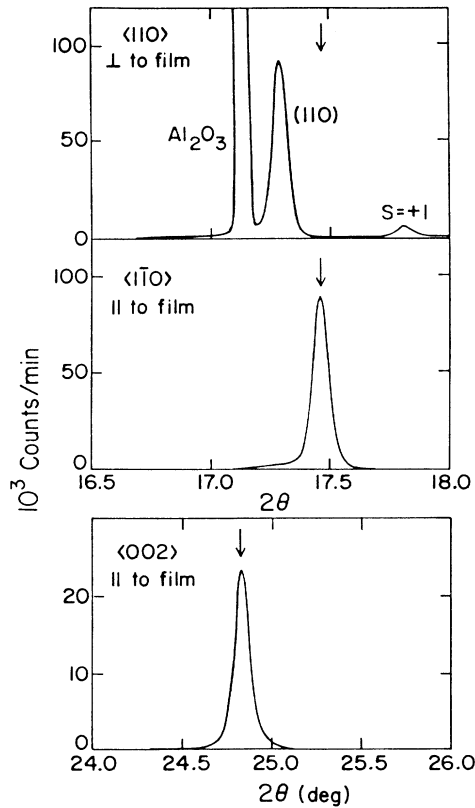


FIG. 2. X-ray diffraction peaks perpendicular and parallel to the film, confirming that the lattice expansion due to hydrogen is only in the normal direction. The arrows indicate the peak positions for the hydrogen-free film (as well as bulk Nb or Ta).

purity for the 85-Å structure and much more,  $\sim 2.5 \mu\Omega \text{ cm}$  per at. % H, for the short-wavelength structure. The rates at 10 K are not significantly different from those at room temperature. For comparison, in bulk Nb and Ta, resistivity increases at the rates<sup>9,10</sup> of  $0.64 \mu\Omega \text{ cm/at. \% H}$ , and  $0.67 \mu\Omega \text{ cm/at. \% H}$ , respectively. We would like to stress that our estimates are subject to an uncertainty with which the volume changes  $\Delta V/V$  are equated to the percentages of dissolved hydrogen. It is clear, however, regardless of this uncertainty, that the hydrogen impurity is much more effective in reducing the mean free path in the 20-Å structure which already started with a somewhat degraded MFP in comparison to the 85-Å sample. Indeed, the degradation of the MFP in the 20-Å structure is so strong that, for the sample loaded with  $\Delta V/V = 0.08$ , below 15 K we observe a logarithmic rise in the resistivity with decreasing temperature, characteristic of two-dimensional weak localization [see inset in Fig. 1(a)].

While most of the samples exhibit smooth curves representing their temperature-dependent resistivity, a sample with the lowest hydrogen content,  $\Delta V/V = 0.013$  in the  $\Lambda = 85 \text{ \AA}$  series, exhibits two distinct anomalies. At 190 K the resistivity drops by about  $1.5 \mu\Omega \text{ cm}$  and at 6.5 K a sudden jump of comparable extent is detected just before the sample goes superconducting. This sample is

perhaps the only one that, at ambient temperature, might be a pure solid solution ( $\alpha$  phase). The anomaly at liquid-helium range has been checked carefully and it appears to be perfectly reversible on cycling between 2–20 K. At this stage, we have no low-temperature x-ray data available to help elucidate the structural character of this sample at helium temperatures. However, a room-temperature x-ray measurement made on this sample after the completion of the low-temperature transport study indicates no changes in diffraction peak widths or shapes.

One of the most interesting features of these measurements is the behavior of the superconducting transition temperatures  $T_c$ , as a function of hydrogen loading (Fig. 3). Both series of samples indicate a rapid suppression of  $T_c$  with increasing hydrogen concentration. This trend is at variance<sup>11</sup> with the effect of hydrogen in bulk Nb or Ta where, within the  $\alpha$ - $\beta$  mixed phase (up to about 0.7 hydrogen fraction) which consists of nearly pure Nb (Ta) together with a segregated hydride,<sup>2,11</sup> the  $\alpha$  phase effectively short-circuits the hydride phase and the  $T_c$  stays constant at the value of hydrogen-free Nb (Ta). When the volume fraction of the hydride phase is so large (above 0.7 hydrogen fraction) that the short-circuiting path is interrupted, the superconducting temperature falls abruptly. The hydride phase is believed not to superconduct above 1.3 K, the lowest temperature investigated in previous studies.

The hydrogen content in all our superlattices, as estimated from Eq. (1), should be well below 0.7 hydrogen fraction, i.e., within the  $\alpha$ - $\beta$  mixed phase as judged by the bulk phase diagram. Assuming for a moment that the  $T_c$ 's of individual Nb and Ta layers comprising our superlattices are affected by hydrogen loading in a way analogous to bulk Nb or Ta, the continuous suppression of  $T_c$  we observe might, at first, be viewed as a direct consequence of the proximity-coupled nature of these multilay-

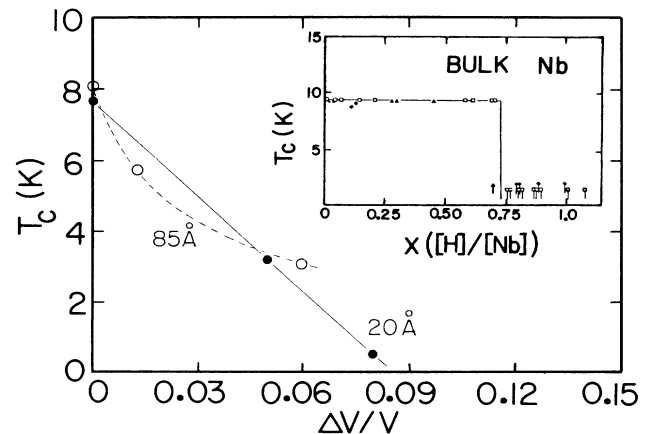


FIG. 3. Superconducting transition temperature  $T_c$  of Nb-Ta superlattices with modulation wavelengths of 85 Å (open circles) and 20 Å (filled circles) as a function of hydrogen loading (solid and dashed curves are guides to the eye). The inset depicts the behavior of  $T_c$  in bulk hydrogenated niobium as determined in Ref. 11.

ers, namely, a weakening of the coupling due to "swelling" of the lower- $T_c$  tantalum spacer. However, since at least three hydrogenated samples have  $T_c$  significantly below 4.4 K ( $T_c$  of bulk Ta), it is unlikely that the weakening of the proximity coupling alone causes degradation of superconductivity.

We therefore believe that the epitaxial constraint responsible for the anisotropic lattice expansion upon hydrogenation alters the phase diagram to such an extent that the superconducting and electronic properties of the individual hydrogenated Nb and Ta layers no longer reflect the properties of their bulk counterparts. As far as superconductivity is concerned, it is likely that the presence of

hydrogen and associated distortion of the cubic cell lead to a gradual suppression of the density of states at the Fermi level. We plan to substantiate this hypothesis with studies on hydrogenated thin epitaxial films of Nb and Ta.

The Nb-Ta superlattices used in this study were kindly provided by Dr. J. E. Cunningham and were prepared in the laboratory of Professor C. P. Flynn. The work of one of us was supported by National Science Foundation, Low Temperature Physics Grant No. DMR-8508392, and the x-ray scattering work was supported by the U. S. Department of Energy, Division of Materials Science, under Contract No. DEAC02-76ER01198.

- 
- <sup>1</sup>P. F. Miceli, H. Zabel, and J. E. Cunningham, Phys. Rev. Lett. **54**, 917 (1985).  
<sup>2</sup>H. Peisl, in *Hydrogen in Metals I*, Topics in Applied Physics, Vol. 28, edited by G. Alefeld and J. Völkl (Springer-Verlag, Berlin, 1978).  
<sup>3</sup>G. T. Meaden, *Electrical Resistance of Metals* (Plenum, New York, 1965).  
<sup>4</sup>A. F. Mayadas, R. B. Laibowitz, and J. J. Cuomo, J. Appl. Phys. **43**, 1287 (1972).  
<sup>5</sup>S. A. Wolf, J. J. Kennedy, and M. Nisenoff, J. Vac. Sci. Tech-

- nol. **13**, 145 (1976).  
<sup>6</sup>J. H. Quateman, Phys. Rev. B **34**, 1948 (1986).  
<sup>7</sup>S. M. Durbin, J. E. Cunningham, and C. P. Flynn, J. Phys. F **12**, L75 (1982).  
<sup>8</sup>P. Miceli, Ph.D. thesis, University of Illinois, Urbana, Illinois, 1987 (unpublished); Miceli *et al.* (unpublished).  
<sup>9</sup>G. Pfeiffer and H. Wipf, J. Phys. F **6**, 167 (1976).  
<sup>10</sup>L. Verdini, J. Less-Common Met. **49**, 329 (1976).  
<sup>11</sup>J.-M. Welter and F. J. Johnen, Z. Phys. B **27**, 227 (1977).